Electronic Supplementary Material (ESI) for Journal of Materials Chemistry

Electrodeposition of luminescent composite metal coatings containing rare-earth phosphor particles

Murugan Ganapathi, Svetlana V. Eliseeva, Neil R. Brooks, Dimitri Soccol,

Jan Fransaer, Koen Binnemans*

Electronic supplementary information (ESI)

Figure S1. Cyclic voltammogram of an electrolyte with composition 0.593:0.391:0.016 mole fractions of acetamide-$DMSO_2$-$NiCl_2$ on a Pt electrode at 130 °C.

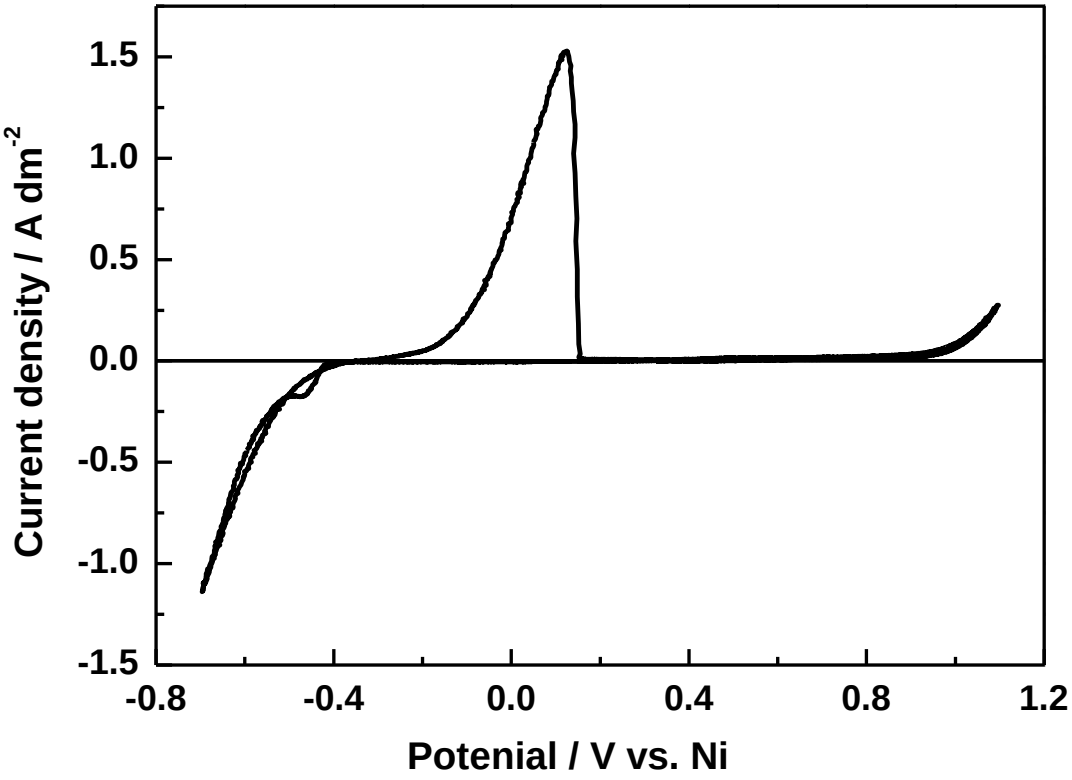

Figure S2. Cyclic voltammogram of an electrolyte with composition 0.617:0.366:0.017 mole fractions of acetamide-$DMSO_2$-$CoCl_2$ on a Pt electrode at 130 °C.

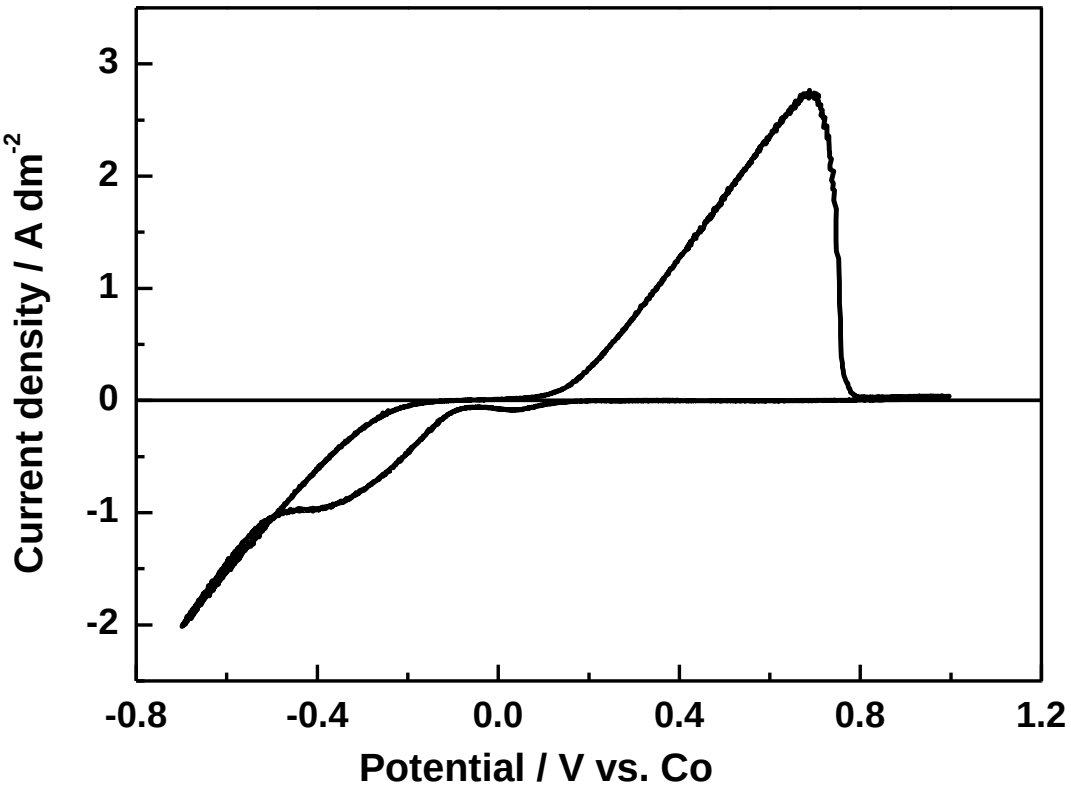

Figure S3. SEM pictures of Ni-Y_2O_3 coatings, electrodeposited from electrolyte solutions with different concentration of Y_2O_3 (For experimental conditions: see Table 1)

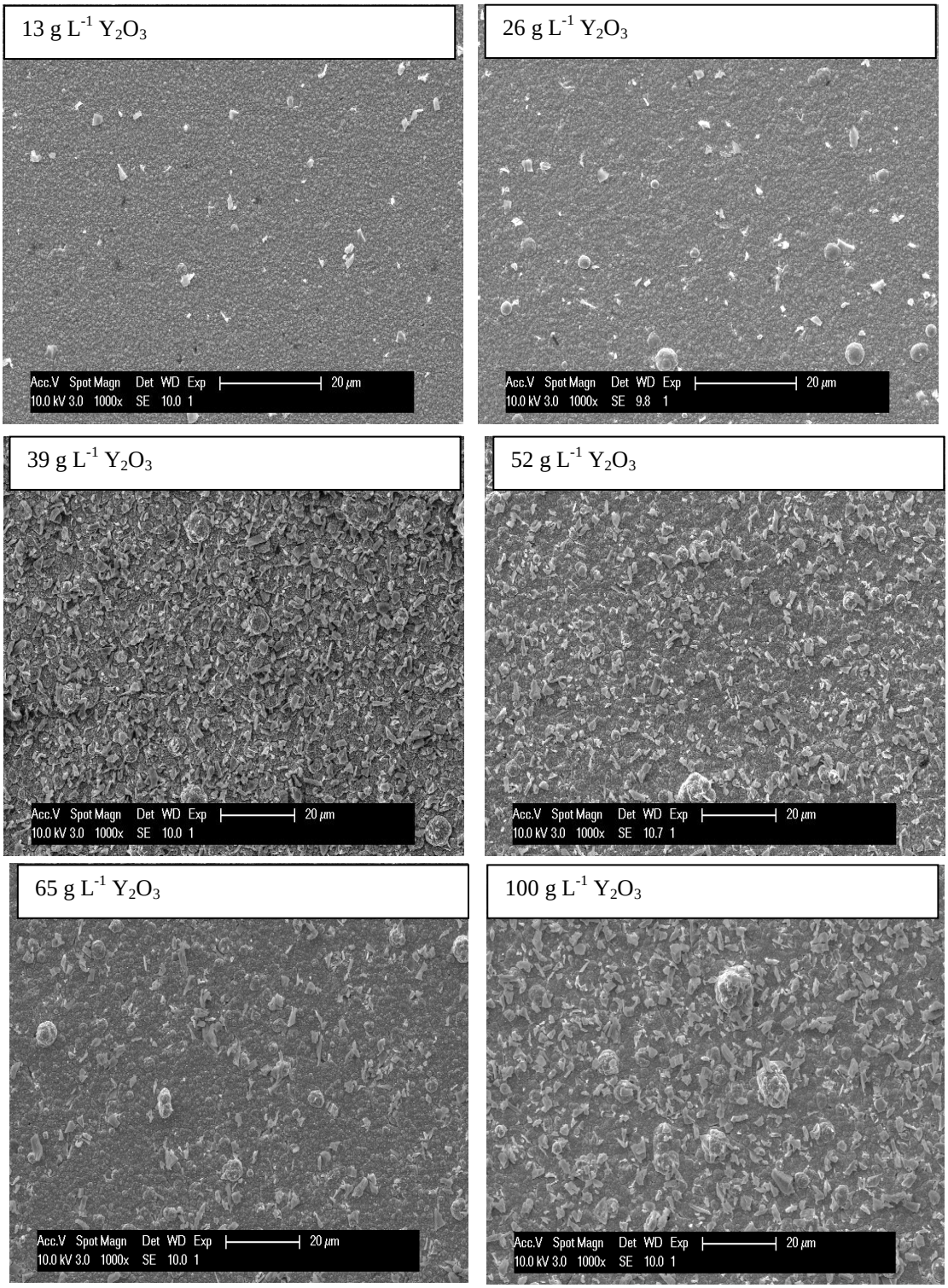

Figure S4. SEM pictures of Ni-Y_2O_3 coatings, electrodeposited from electrolyte solutions with different concentration of Y_2O_3 (For experimental conditions: see Table 1). The coatings are the same as those shown in Figure S3, but at a different magnification.

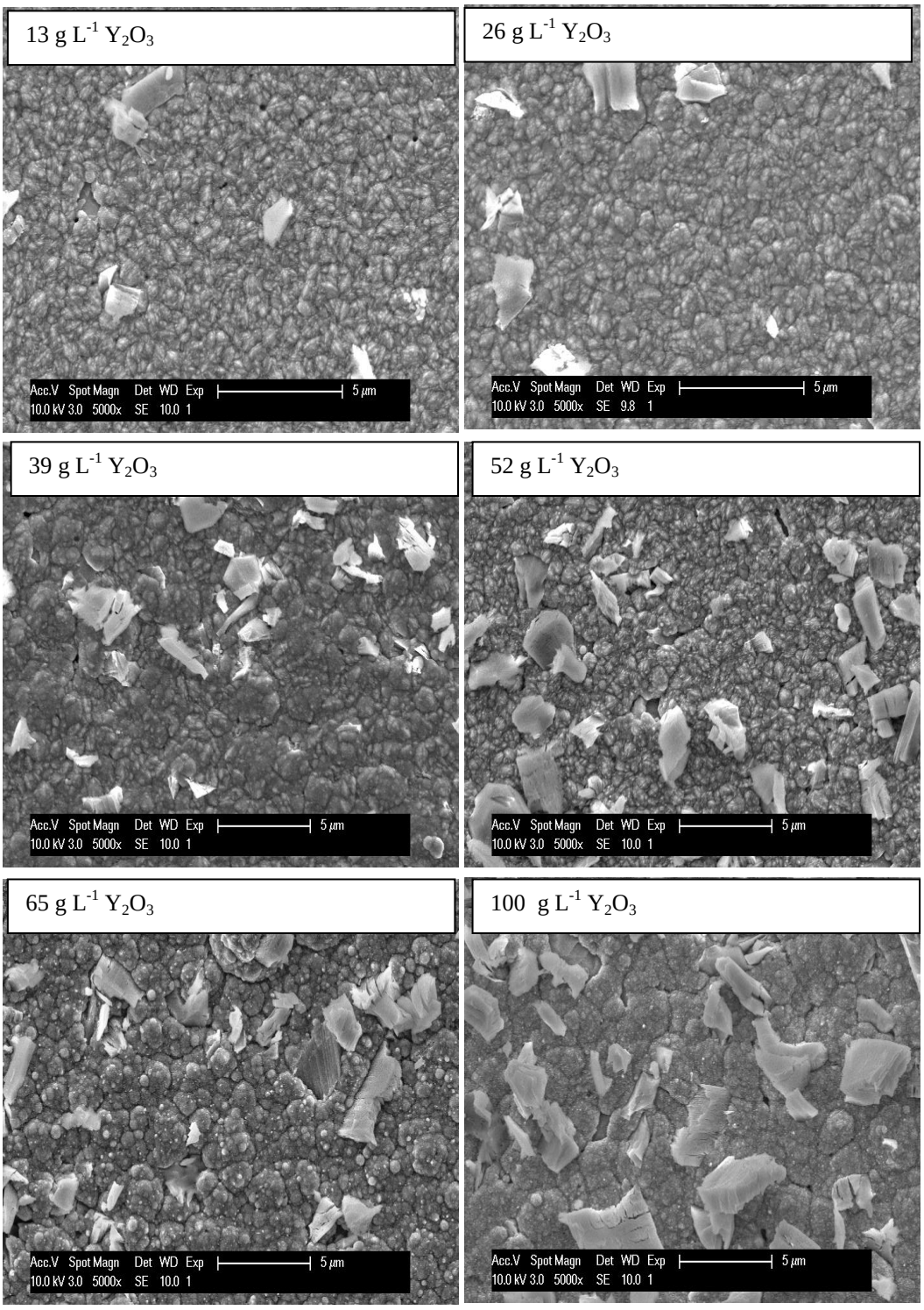

Table S1. Effect of the deposition potential on the loading of Y_2O_3 particles (at 130 °C).

Potential vs. Ni (V)	atomic % of O	atomic % of Y	atomic % of Ni	vol. % of Y_2O_3
-0.2	14.5	9.1	76.4	29
-0.4	19.4	15.6	65.0	45
-0.8	19.4	15.3	65.3	45

Table S2. Influence of temperature on Y_2O_3 codeposition in nickel.[a]

temperature (°C)	atomic % of O	atomic % of Y	atomic % of Ni	vol. % of Y_2O_3
130	19.5	15.5	65.0	45
150	15.3	11.3	73.4	35

[a] Deposits obtained at -0.4 V vs. Ni, with stirring (250 rpm), in an electrolyte bath with 100 g L^{-1} of Y_2O_3.

Figure S5. Effect of the deposition potential on the morphology of Ni-Y_2O_3 coatings obtained at 130 °C (SEM pictures at two different magnifications, left and right).

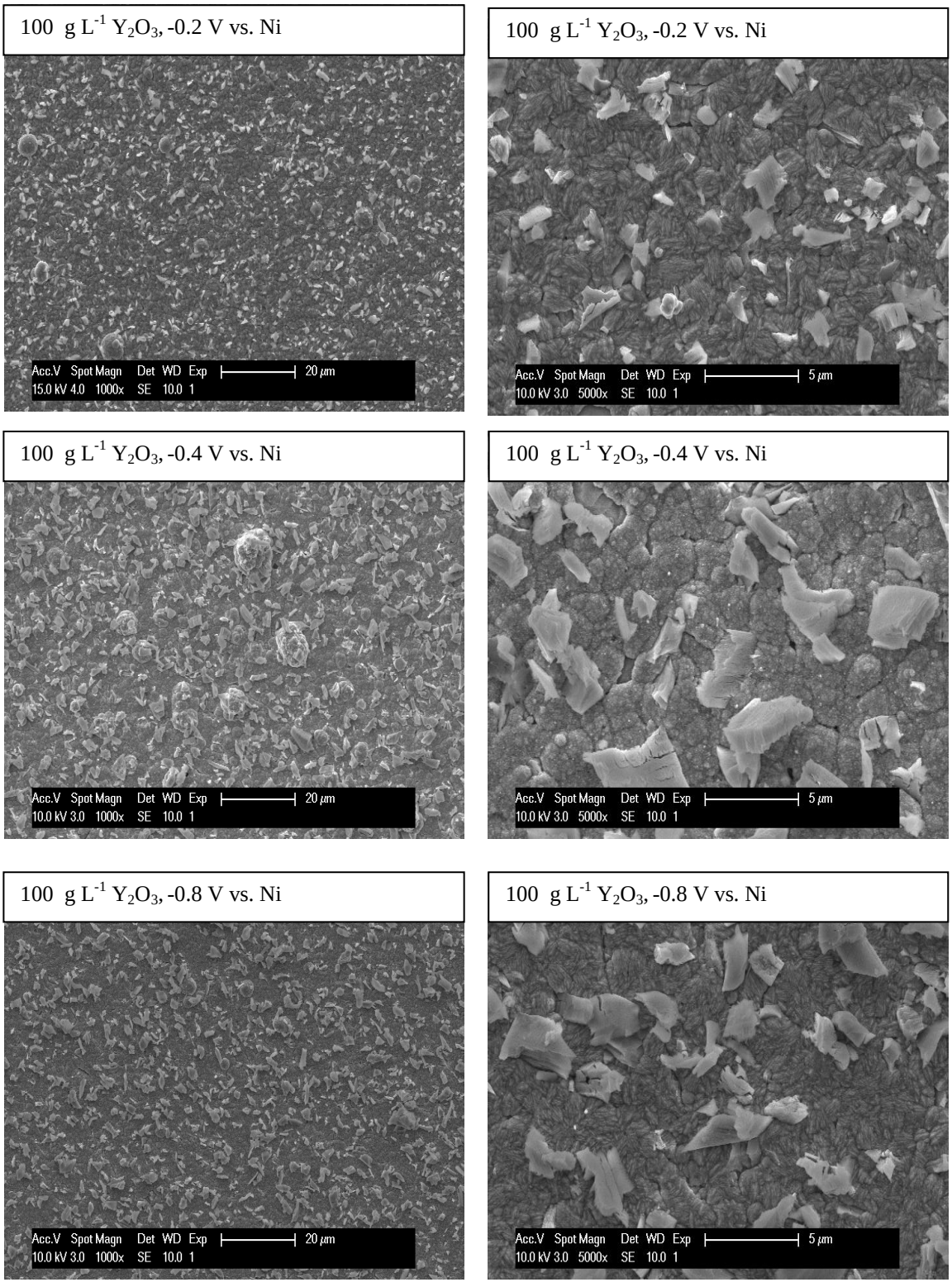

Figure S6. Influence of temperature on Y_2O_3 codeposition in nickel. SEM pictures (left) and EDX spectra (right).

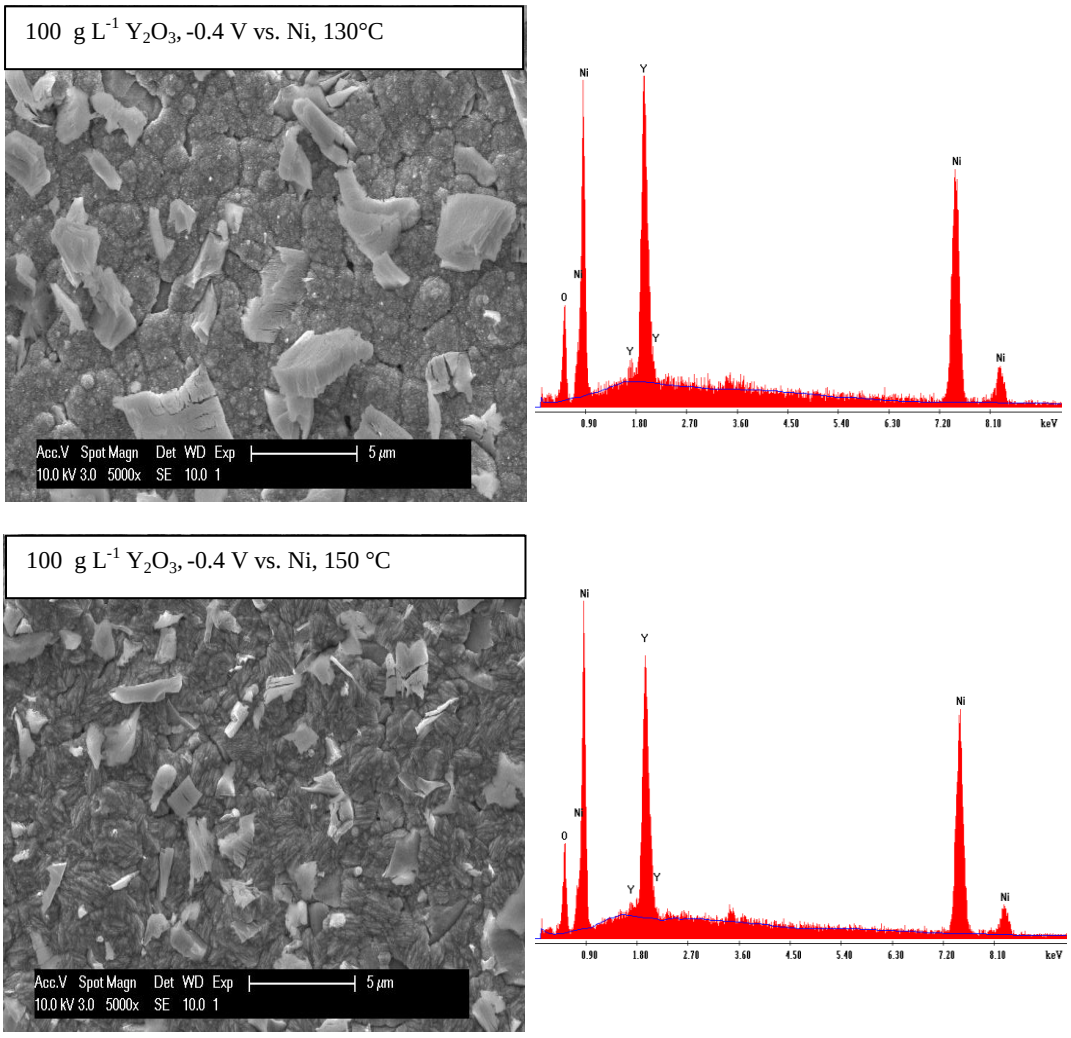

Figure S7. SEM pictures of Co-Y_2O_3 coatings, electrodeposited from acetamide:$DMSO_2$:$CoCl_2$ electrolyte solutions with different concentration of Y_2O_3, and different deposition potentials.

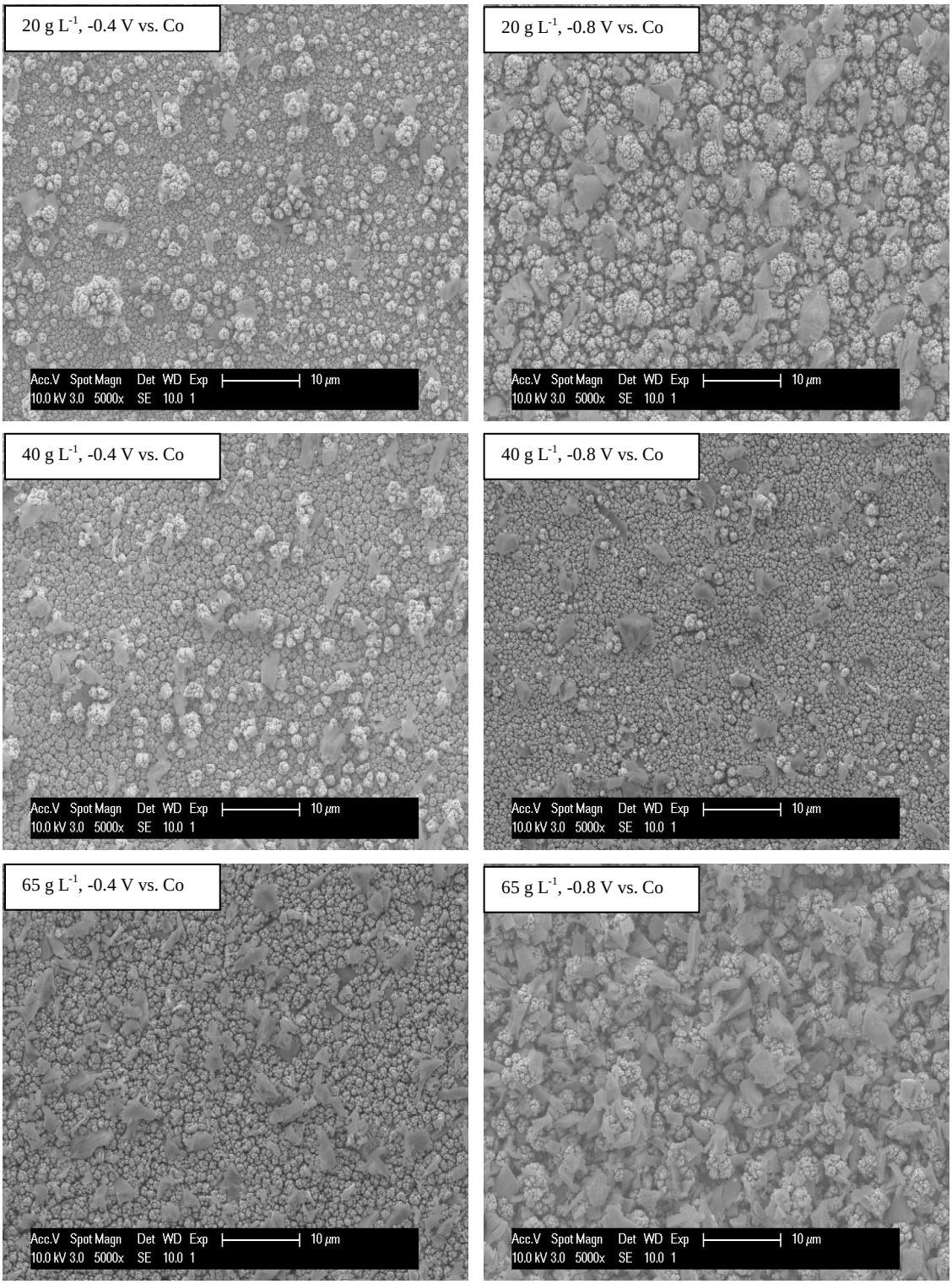

Figure S8. EDX spectrum of a Co-Y_2O_3 coating.

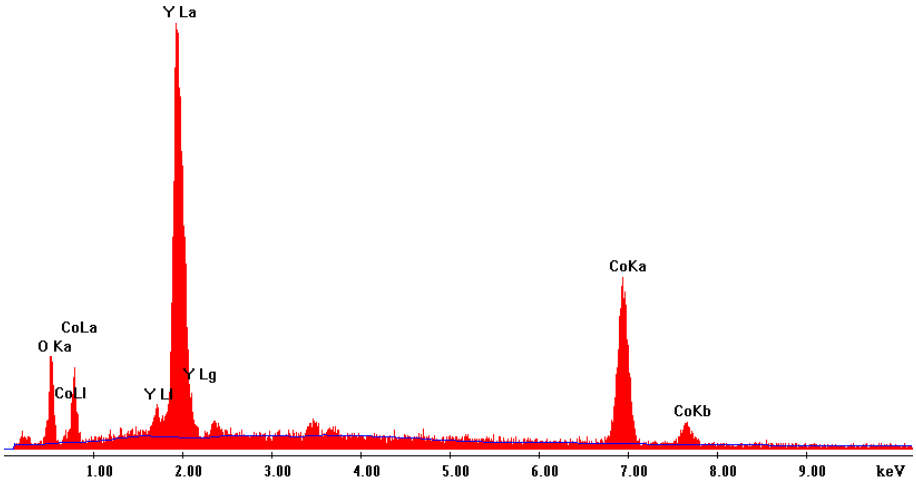

Figure S9. SEM pictures of: (a) Ni coatings with Y_2O_3:Eu^{3+} phosphor particles, and (c) Ni coatings with Gd_2O_2S:Tb^{3+} phosphor particles, deposited at -0.4 V vs. Ni at the temperature of 130 °C . The electrolyte was stirred at 250 rpm. (b) and (d) are the EDX spectra of (a) and (c), respectively.

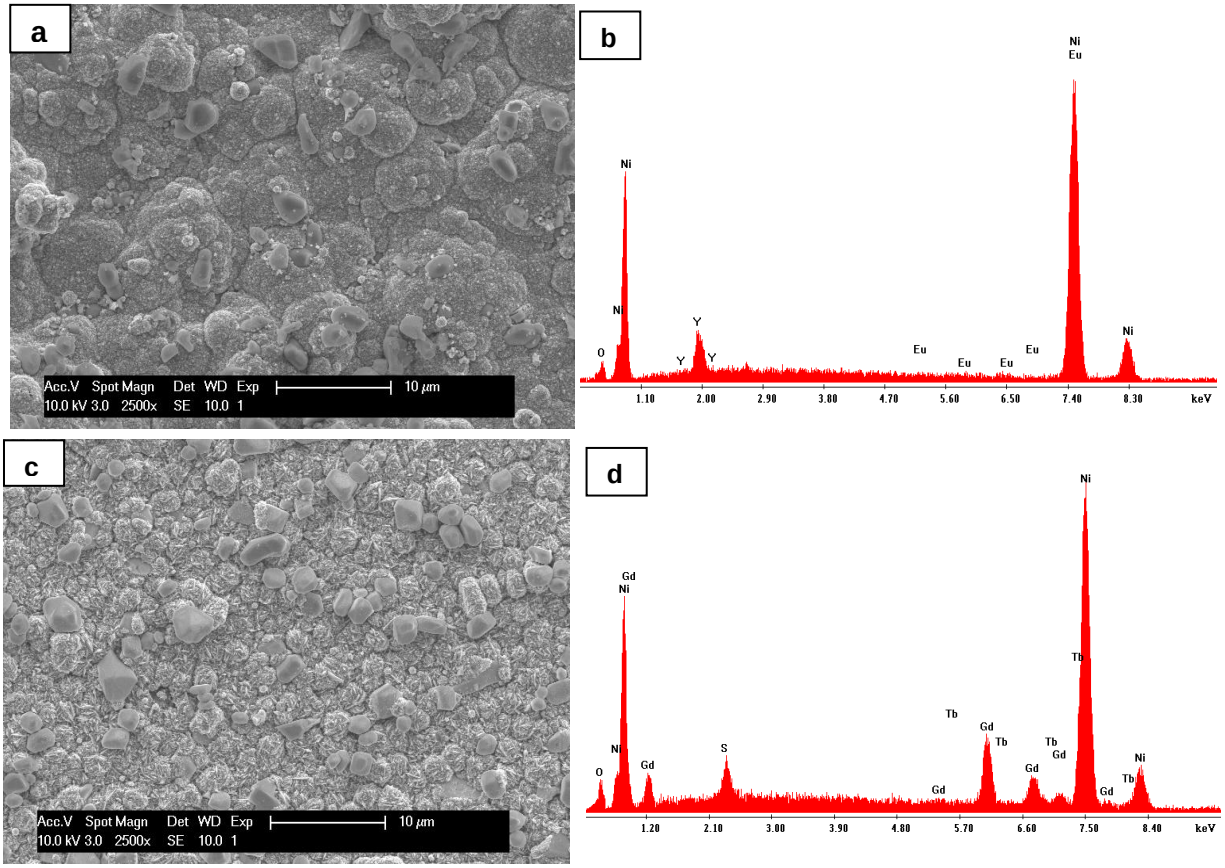

Figure S10. SEM pictures of: (a) Ni coatings with $BaMg_2Al_{16}O_{27}:Eu^{2+}$ phosphor particles, and (c) Ni coatings with $Y_3Al_5O_{12}:Ce^{3+}$ phosphor particles, deposited at -0.4 V vs. Ni at the temperature of 130 °C . The electrolyte was stirred at 250 rpm. (b) and (d) are the EDX spectra of (a) and (c), respectively.

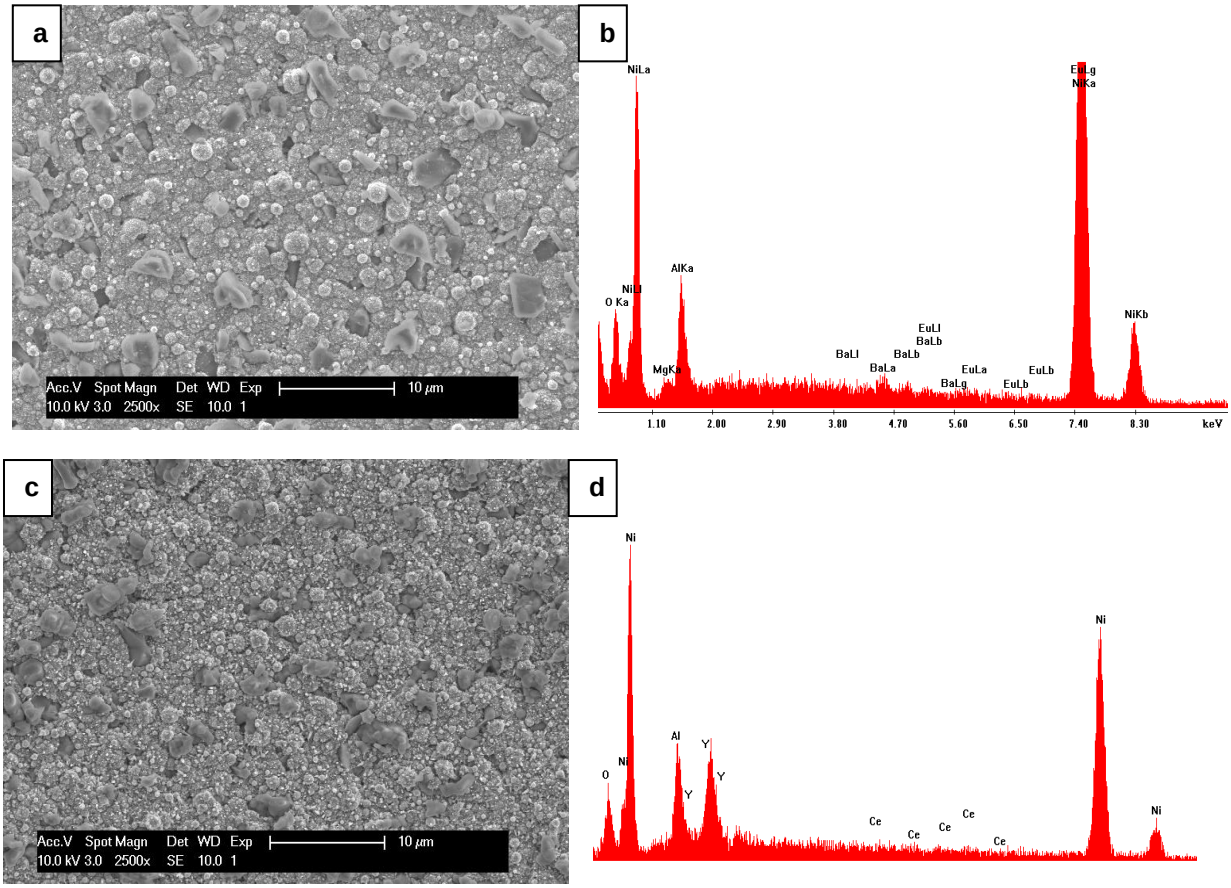

Figure S11. Excitation spectra of Eu_2O_3 powder (λ_{em} = 611 nm) as a function of the thickness of the powder layer.

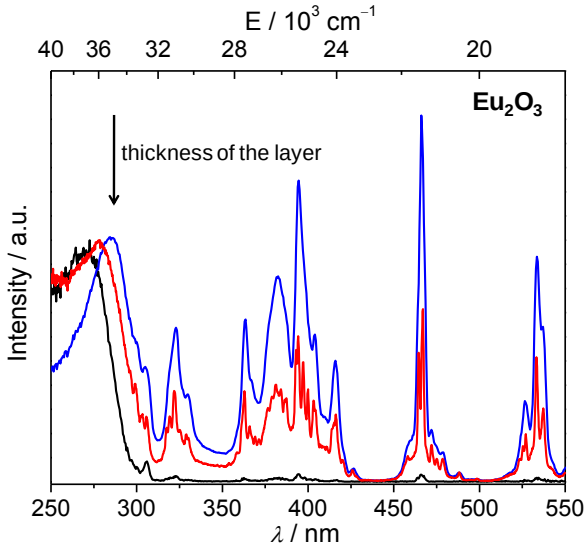

Figure S12. Excitation spectra of $Gd_2O_2S:Tb^{3+}$ powder (λ_{em} = 545 nm) as a function of the thickness of the powder layer.

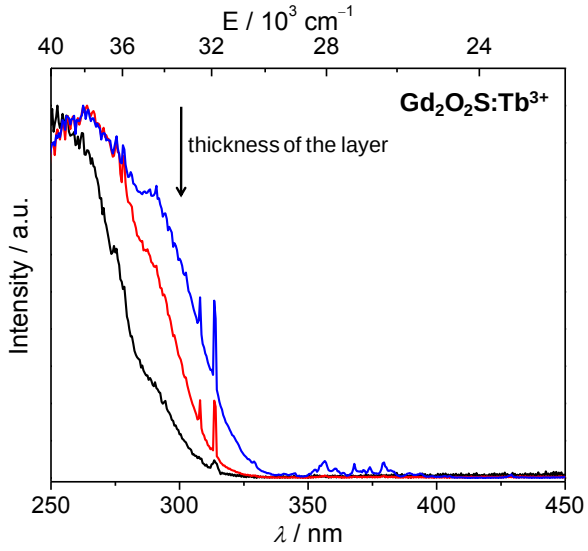

Figure S13. Pictures of a nickel coating with $Y_3Al_5O_{12}:Ce^{3+}$ phosphor particles, illuminated (a) by daylight and (b) with UV radiation of 340 nm.

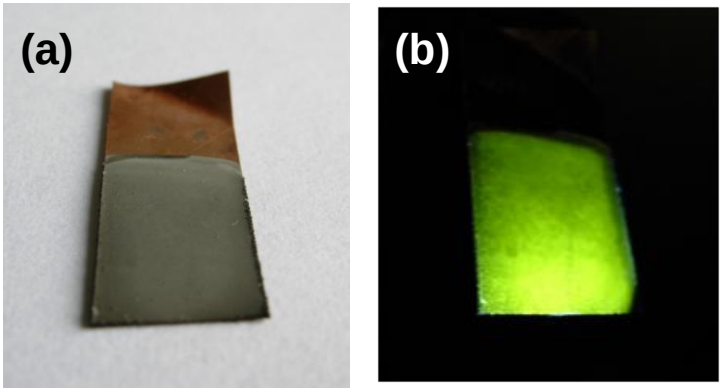

Figure S14. Room temperature luminescence spectra of $Y_3Al_5O_{12}:Ce^{3+}$ excited at different wavelengths.

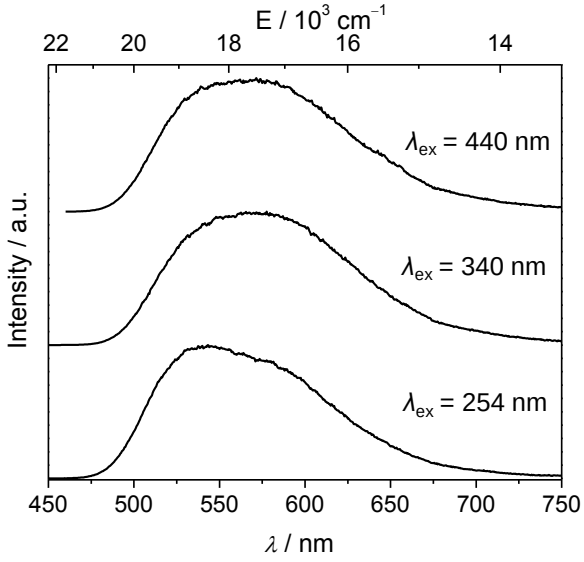

Figure S15. Room temperature emission spectra under excitation at 254 nm of the mixtures of red (Y_2O_3:Eu^{3+}) and green (Gd_2O_2S:Tb^{3+}) phosphors in (a) 90:10, (b) 75:25, (c) 50:50, (d) 25:75 and (e) 10:90 wt.% ratio, respectively.

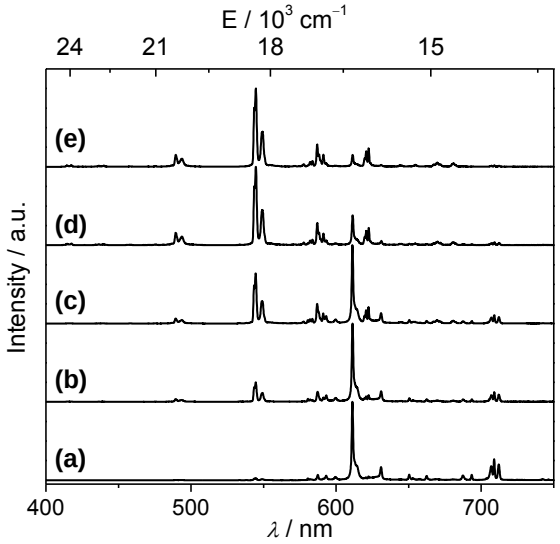

Table S3. Luminescence lifetimes (τ_{obs}, ms) of Eu($^5D_0$) and Tb($^5D_4$) levels for red (Y_2O_3:Eu^{3+}) and green (Gd_2O_2S:Tb^{3+}) phosphors, the mixtures of them and the corresponding composite Ni coatings.

Ratio Eu:Tb / wt. %	State	Eu($^5D_0$)	Tb($^5D_4$)
100:0	powder	1.04(1)	-
	Ni coating	1.04(1)	-
90:10	powder	1.03(1)	0.57(1)
75:25	powder	1.02(1)	0.56(1)
	Ni coating	1.00(1)	0.56(1)
50:50	powder	1.03(1)	0.56(1)
	Ni coating	1.02(1)	0.58(1)
25:75	powder	1.02(1)	0.58(1)
	Ni coating	1.00(1)	0.57(1)
10:90	powder	1.02(1)	0.57(1)
0:100	powder	-	0.55(1)
	Ni coating	-	0.55(1)

Table S4. CIE coordinates of the red ($Y_2O_3:Eu^{3+}$) and green ($Gd_2O_2S:Tb^{3+}$) phosphors, the mixtures of them and the corresponding composite Ni coatings.

Ratio Eu:Tb / wt. %	State	(*x*; *y*)
100:0	powder	0.652; 0.345
	Ni coating	0.638; 0.346
75:25	powder	0.563; 0.408
	Ni coating	0.578; 0.401
50:50	powder	0.515; 0.464
	Ni coating	0.489; 0.471
25:75	powder	0.414; 0.522
	Ni coating	0.410: 0.523
0:100	powder	0.411; 0.537
	Ni coating	0.373; 0.568

Figure S16. Room-temperature emission spectra of (a) the 50:50 wt.% mixture of blue and yellow phosphors and (b) the corresponding Ni coating. Black lines: λ_{ex} = 254 nm, green lines: λ_{ex} = 340 nm.

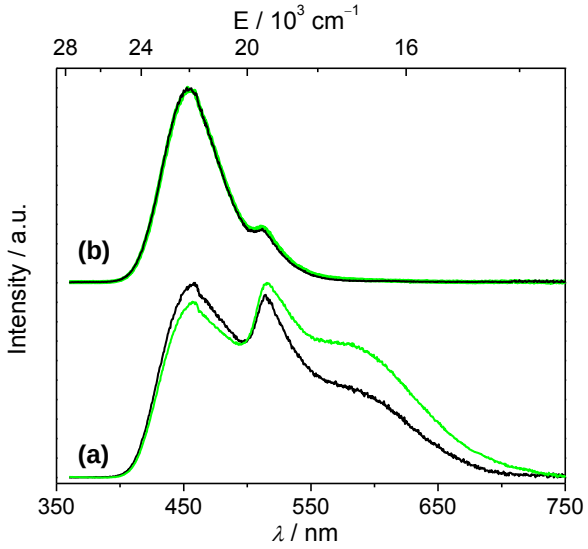

Figure S17. (Left) Photograph of the powder of 50:50 wt.% mixture of yellow (YAG: Ce^{3+}) and blue (BAM: Eu^{2+}) phosphors and the corresponding composite Ni coating under 254 nm excitation and (right) CIE trichromatic coordinates (circles: powder, triangles: Ni coating; black: λ_{ex} = 254 nm, red: λ_{ex} = 340 nm).

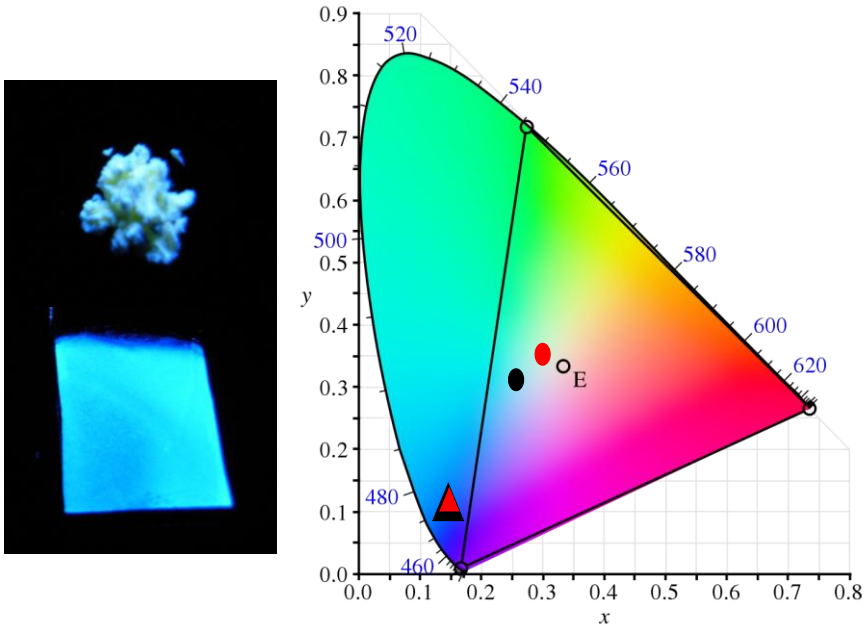

Figure S18. SEM pictures (two different magnifications) and EDX spectrum of binary mixtures of the red (Y_2O_3:Eu^{3+}) and green (Gd_2O_2S:Tb^{3+}) phosphors, co-deposited with Ni at -0.4 V vs. Ni.